External sulfate attack in structural concrete made with Portland-limestone cement: an experimental study

Nicola Cefis[1], Cristina Tedeschi[2], Claudia Comi[3]

Department of Civil and Environmental Engineering
Politecnico di Milano
Piazza Leonardo da Vinci, 32, 20133 Milano (Italy)
[1] nicola.cefis@polimi.it, [2]cristina.tedeschi@polimi.it, [3]claudia.comi@polimi.it

Abstract

This experimental study aims to assess the effect of external sulfate attack on structural concrete made with a common Portland-limestone cement. The experimental campaign, lasted about three years, has been performed on standard-sized cylinders (⌀15×30 cm) subject to different exposure conditions. The overall swelling of the specimens due to chemical reactions was monitored in time. SEM-EDS observations and XRD tests were also carried out. Results showed the presence of secondary ettringite causing swelling and micro-cracks formation. The porosity increase due to sulfate attack of the outer skin of the specimens was measured. Ultrasonic measurements and compression tests on cores drilled from the cylinders immersed in different solutions allowed to confirm and quantify the consequent degradation of macroscopic elastic properties.

Keywords

Concrete; Sulfate attack; Delayed ettringite formation; Damage

1 Introduction

The sulfate attack (SA) is one of the phenomena that can affect the durability of concrete structures in contact with sulfate-rich soils or water, see e.g.

Alexander et al. (2013), Skalny et al. (2002). An adequate simulation of the behavior of these structures requires a reliable characterization of the swelling and degradation which may occur in concrete due to the chemical reactions between the cement paste and the sulfates diffusing in the material through its porous microstructure. These reactions lead to the formation of gypsum, secondary ettringite and thaumasite with consequent expansion and micro-cracks formation in the hardened concrete. The Thaumasite Sulfate Attack leads to dissolution of the main phases of the hydrated cement and to disintegration of concrete. The ettringite formation is less destructive, it leads to expansion and consequent cracks formation in concrete.

The extent and the kinetics of the chemical reactions are strongly dependent on the mineralogical composition of the cement, on the concrete properties (porosity, aggregates size, aggregate composition,...) and environmental conditions (temperature, aggressive solution composition,...) and there is some controversy on the explanation of the exact mechanism of expansion and degradation, see e.g. the review article of Neville (2004). Also the influence of the temperature on the phenomenon is not fully clarified. While it is widely recognized that low temperature (below $15°C$) favors the thaumasite formation (Ramezanianpour and Hooton (2013), Kakali et al. (2003)) and that at room temperature ettringite prevails, several experimental evidences of thaumasite formation at temperature above $20°C$ are reported e.g. in Brown and Hooton (2002), Bassuoni and Nehdi (2009), Rahman and Bassuoni (2014). The knowledge of the actual expansion and damage is of paramount importance to identify the material parameters intervening in the various mechanical models proposed to simulate the effect of the sulfate attack, as those formulated by Tixier and Mobasher (2003), Idiart et al. (2011), Cefis and Comi (2014).

In view of the complexity of the phenomenon, many experimental campaigns were carried out to investigate the different aspects of the external sulfate attack on the cement paste (Planel et al. (2006)), on mortar (Akpinar and Casanova (2010),Yu et al. (2013), Santhanam et al. (2003), Chen and Jiang

(2009), El-Hachem et al. (2012)) and on concrete (Park et al. (1999), Ouyang et al. (2014),Shamaa et al. (2015)). The effect of different cements composition on the durability of mortar and concrete specimens was experimentally studied in Roziere et al. (2009) through expansion measurements and SEM observations. This extensive experimental campaign considered cements of class CEM I and CEM III, according to the European code EN197-1:2011 (2011). The beneficial effect of volcanic ash addition to ordinary Portland cement was proved in Naseer et al. (2008). In Park et al. (1999) the compressive strength reduction of concrete specimens exposed to SA was measured, while in Ouyang et al. (2014) the degradation was quantified through hardness measures. In both cases an ordinary Portland cement, CEM I, was used in the concrete mix design. Again considering CEM I, in Boyd and Mindess (2004) compression and tension tests showed that the sulfate attack induces a tensile strength reduction faster than the compressive strength reduction; recently, in Haufe and Vollpracht (2019), the tensile strength was measured on briquet specimens after half year of exposure to sulfates and the influence of the C_3A content was evidenced; in Shamaa et al. (2015) the effect of the moisture conditions on concrete made by ordinary Portland cement was studied. The coupled effect of mechanical loading, SA and dry-wet cycles was recently studied on fly-ash slag concrete in Gong et al. (2019).

The present experimental campaign is aimed to investigate the resistance to external sulfate attack of structural concrete, made with a Portland-limestone cement, CEM II A-LL. It should be remarked that this cement, even though not classified as sulfate resisting in the European code EN $197-1:2011$, is considered as sulfate resisting by Italian National Standards UNI9156:2015 (2015) and Portuguese National Standards NPEN206-1:2007 (2007), and hence it is very commonly used also in moderately aggressive environmental conditions. Brown and Hooton (2002), however, showed that also in concrete prepared using sulfate-resisting cements, after two decades of immersion in sulfate solution, there is evidence of ettringite and thaumasite formation. More recently, Loser

and Leemann (2016) showed, by new accelerated tests, that concrete made with CEM II A-LL exposed to cycles of immersion in sulfate solution followed by drying exhibited a significant expansion and stiffness reduction. It is therefore of particular interest to assess experimentally the resistance to sulfate attack of concrete made with this cement. The present paper reports the results of an experimental campaign focused on this and lasted three years. The concrete considered, made with cement with low C_3A content ($< 8\%$) and low water-to-cement (w/c) content (≤ 0.45) falls inside the "safe zone" where failure did not occur within 40-years exposure period, as defined in Monteiro and Kurtis (2003). Nevertheless, even in this zone, SA leads to some degradation which is worth investigating. In particular the experimental quantification, in long term tests, of the mechanical effects of SA in terms of the reduction of strength and stiffness for concrete made with CEM II A-LL still lacks. The experimental campaign here reported is aimed to provide some data in this direction.

To this purpose, concrete specimens prepared using CEM II A-LL were immersed in solutions with different concentrations of sodium sulfate Na_2SO_4 for almost three years. Several different complementary aspects have been considered to determine the effects of SA; both local chemo-physical measurements in the mortar around the large-size aggregates and global mechanical measures on the concrete specimens have been performed using different techniques. SEM images, energy dispersive X-ray spectrometry (EDS) and X-ray diffraction (XRD) allowed to evidence the presence of secondary ettringite in the outer parts of the specimens exposed to the aggressive solutions. Porosimetry measurements were also performed. The evolution of the reaction and the consequent influence on the mechanical behavior of the material were monitored by measuring the longitudinal and radial expansions and the variation of mass. After about three years of immersion some cores were drilled and tested in uniaxial compression. The Young modulus measured from the mechanical tests was compared with that indirectly measured through ultrasonic wave propagation tests.

Table 1: Phase composition of cement

Cement	C_3A	C_4AF	C_3S	C_2S
CEM II/A-LL 42.5R	6.08%	7.90%	34.71%	24.04%

2 Materials, casting and curing

The experimental campaign of this study has been conducted on concrete cylindrical specimens of diameter 15 cm and height 30 cm, prepared with a concrete mix design characterized by 0.45 water to cement ratio, 250 Kg/m^3 cement content and 3. cm maximum aggregate size. The aggregates employed are siliceous, non-reactive with respect to alkali-silica reaction to avoid coupled effects of SA and degradation induced by the alkali-silica reaction. The cement used is Portland limestone cement CEMII / A-LL, with 20% of limestone of high $CaCO_3$ content, its chemical composition is given in Table 1. Standard cubes of 15 cm side have also been produced to assess the mechanical strength of the material at 28 days.

The cylinders and the cubes were cast in steel molds and cured in a climatic chamber at controlled temperature ($T = 20^\circ\ C$) and humidity ($RH = 90\%$) for 28 days. After curing, the mean compressive strength, obtained by mechanical tests on 6 cubes, was 30 MPa.

3 Experimental procedure

After curing brass studs with a small central hole, were glued on cylinders for the subsequent measurement of axial and longitudinal expansion. Twelve studs were placed on each cylinder, 4 at 90 degrees one from each other at 3 different heights, see Figure 1.

Then the specimens have been fully immersed in different solutions in order to determine the response of the material in different environmental situations. Twelve cylinders and six cubes were fully immersed in big containers with three different solutions: demineralized water and solutions of demineralized water

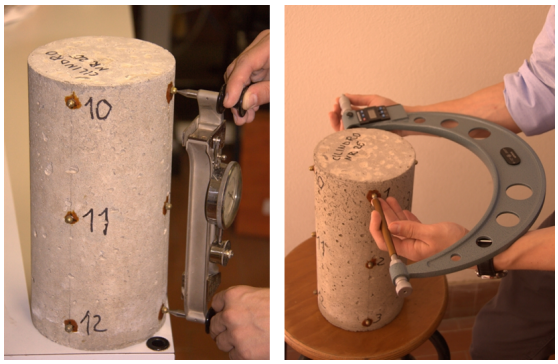

Figure 1: Measure of longitudinal and radial expansions

with 5% and 10% of sodium sulfate. The baths were covered in order to minimize evaporation. Two cylinders were stored in air in a climatic chamber at temperature $T = 20°\ C$ and $RH = 50\%$ to provide reference data in neutral conditions.

Measurements were performed initially every 14 days to accurately capture the phenomenon of water absorption. Full saturation was reached in all specimens after about 90 days; after saturation, measurements were performed every two months with the following procedure. Each specimen was extracted from the solution and, after a couple of minutes necessary to allow dripping of the solution in excess, it was weighed. After weighing, the distances between the studs were measured. The measurements in the longitudinal direction were performed with a mechanical comparator Huggenberger, while the distances in the radial direction were measured with a electronic micrometer Mitutoyo, see Fig. 1. The variation of these distances allowed to compute the longitudinal and radial strains.

After 400 days of exposure, in order to identify the morphology and the modifications due to the sulfate attack a series of observations with Scanning Electron Microscopy (SEM) and Energy Dispersive X-ray Spectrometry (EDS) were performed. The observations were carried out through microscope MIRA3XMU at the Department of Earth Sciences of the University of Pavia. The samples were immersed into a graphite substrate through a physical vapor deposition

process and then observed at the microscope. The morphology SEM-EDS were performed on sawed, not polished sections.

At the same time, samples of the mortar matrix were extracted from different locations of a concrete specimen and subjected to X-Ray diffraction measurements.

After 600 days of immersion, porosity measurements were conducted through a Micromeritics AutoPore IV 9500 series mercury intrusion porosimeter (MIP). In this study a measuring pressure from 0.15 to 33000 psia was applied to mortar samples, of dimensions $15mm \times 15mm \times 20mm$, taken from the concrete cylinders.

Finally, after about three years of immersion cores of 5 cm diameter were drilled from 3 cylinders (exposed to different solutions). To determine the effect of sulfate penetration, for each cylinder, two cores were drilled near the surface while one was drilled at the center. From each one of the 9 cores two cylindrical specimens (⌀5×11 cm) were obtained and tested in uniaxial compression conditions.

4 Results of local chemo-physical material characterization

4.1 SEM-EDS observations

One cube stored in sodium sulfate solution at 10% was extracted from the solution after 400 days in order to identify the portion reached by the aggressive solution and to obtain samples of material affected and unaffected by SA. The cube was cut and stored in the climatic chamber at $RH = 50\%$ and $T = 20°C$. The evaporation of water led to the crystallization of salt, making visible a central core free of salt and a penetration zone about 8 mm thick. The observations concerned three small samples taken from the above mentioned

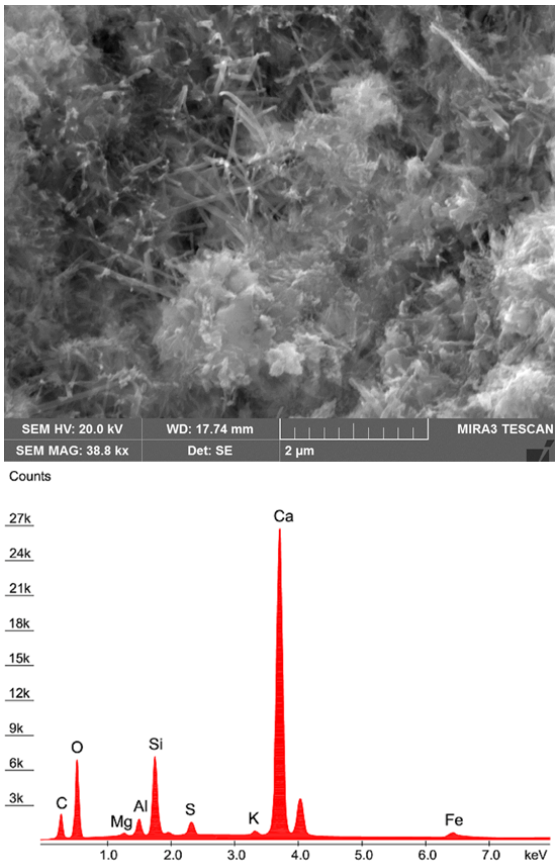

Figure 2: Hydrated matrix in sample 1: SEM image and EDS spectrum

cube and from a reference specimen:

- Sample 1: taken from the reference concrete specimen stored in the climatic chamber at $T = 20°C$ and $RH = 50\%$ and not subject to sulfate attack. The purpose of these observations was the identification of the phases naturally produced during the hydration of the cement.

- Sample 2: taken from the external part of the cube immersed in the 10% solution of sodium sulfate for 400 days. The purpose of these observations was to evaluate the microstructural alterations and the ettringite formation due to the penetration of sulfate ions and the reaction with the calcium aluminates.

- Sample 3: Taken from the middle part of the same cube of sample 2. These further observations were aimed to evaluate the microstructure of a portion of the material immersed in the aggressive solution but not yet directly affected by the reaction with the sulfates.

The observations conducted on the sample 1 showed the typical morphology of the cement paste. Most of the material is made of the amorphous gel of calcium silicate hydrates, with rare formations of primary ettringite incorporated in the gel.

The primary ettringite, with the typical needle-like shape, can be seen in the SEM image of Figure 2. The corresponding EDS spectrum shows a predominant presence of calcium silicate hydrates (indicated by the main peaks of silicon and calcium in the spectrum) and a limited presence of the ettringite components (peaks of aluminum and sulfur). Figure 3 shows a SEM image (magnification 26400×) of sample 2 where a crack is visible. The crack is filled by an expansive phase. The EDS spectra centered at points 1 and 2 of Figure 3, i.e. inside the crack and at the edge of the crack, are reported in the same figure. One can remark that the crystals inside the crack are rich in sulfur, which probably indicates the presence of ettringite, while the matrix at the edge is rich in silicon, besides that in calcium, as typical in *C-S-H* gel.

One should remark that the EDS spectrum of point 1 is also compatible with the presence of a thaumasite-ettringite mix as shown e.g. in Brown and Hooton (2002). In our case, however, the visual inspection of the concrete specimen which did not appeared seriously degradated and the XRD analyses seem to indicate the formation of ettringite only.

Figure 4 shows the SEM image and EDS spectrum for sample 3, mainly composed of calcium silicate hydrates with a limited amount of ettringite. The EDS spectrum shows a limited amount of sulfur and is similar to that of sample 1, see Fig. 2. This confirms that the internal part of the specimen was not yet reached by the sulfate attack.

To sum up, the observations by SEM showed the presence of a newly formed

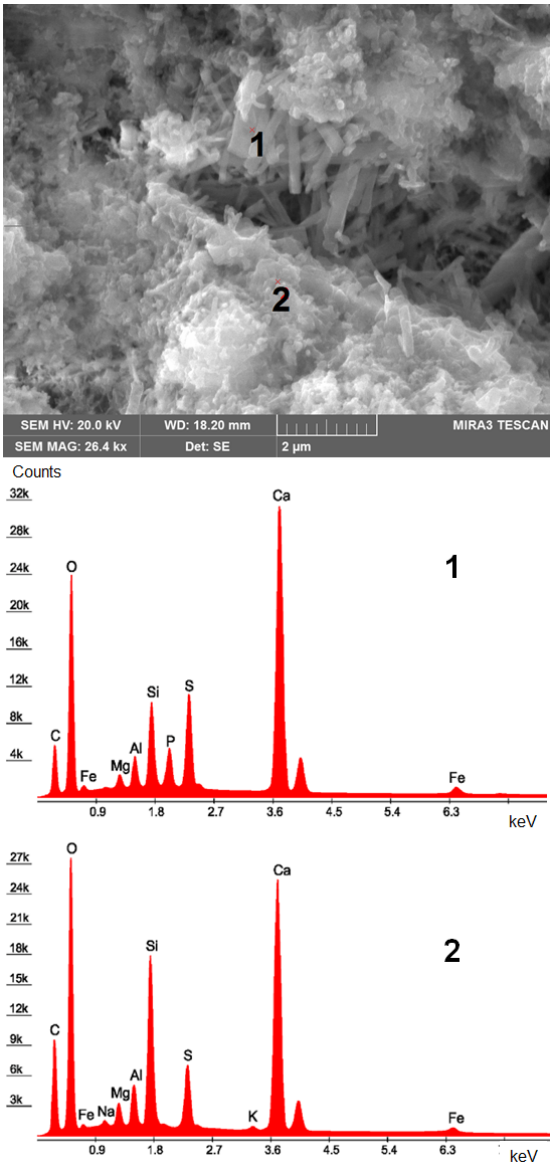

Figure 3: SEM image of a crack in Sample 2 and EDS of points 1 and 2, inside and outside the crack, respectively

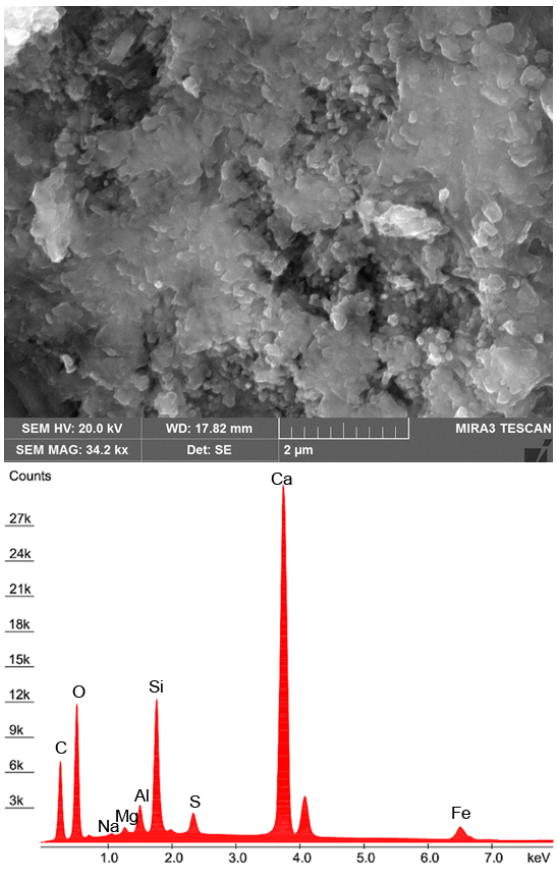

Figure 4: Amorphous phase in sample 3: SEM image and EDS spectrum

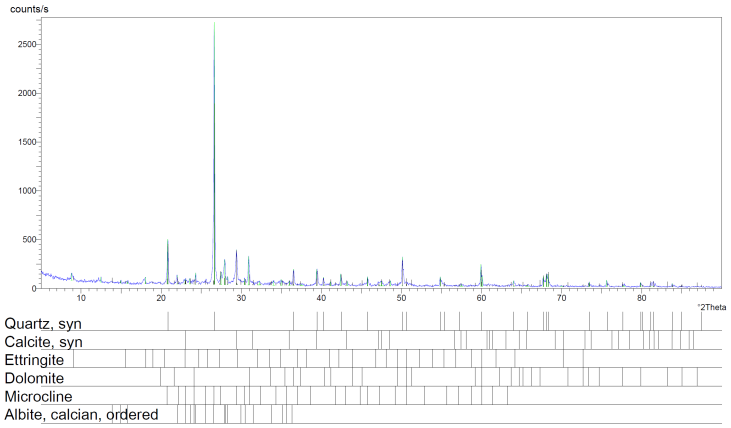

Figure 5: XRD of mortar powder of the external part of the specimen after 400 days of immersion in 10% sodium sulfate solution

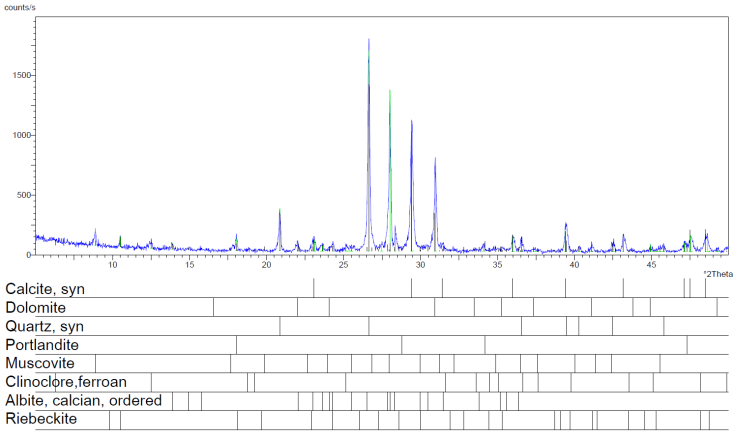

Figure 6: XRD of mortar powder of the central part of the specimen after 400 days of immersion in 10% sodium sulfate solution

crystalline phase in the external part of the specimen immersed in sodium sulfate solution. Through EDS spectra and XRD analyses, reported in the following subsection, this new phase could be recognized as secondary ettringite. On the contrary no delayed ettringite formation was observed in the internal part of the specimen.

4.2 X-Ray Diffraction

X-Ray diffraction measurements have been carried out on two samples taken from the same cube used in SEM-EDS measurements. One of the samples was taken near the surface, in the region affected by the SA and the other sample was taken in the center of the specimen which was not reached by the penetrating sulfates. Figure 5 shows the result of the test on the first sample. Besides the minerals of the aggregates (quartz, calcite, dolomite), ettringite has been clearly identified and is reported in the table of constituents, no thaumasite has been identified.

Figure 6 reports the results of the XRD of the sample taken from the central part of the cube. In this case ettringite was not detected. This indicates that the amount of ettringite possibly present was below the sensitivity of the XRD measurements.

4.3 Porosity measurements

After 600 days of immersion, five different samples of mortar have been examined: sample A, taken from a cylinder immersed in pure water; samples B and C taken, respectively, from the central part and near the surface of a cylinder immersed in 5% sodium sulfate solution; and samples D and E taken, respectively, from the central part and near the surface of a cylinder immersed in 10% sodium sulfate solution.

Figure 7 shows the values of the porosity and of the mass density obtained. The porosity of the material in contact with the aggressive solutions, samples C and E, is higher than that in the central part of the specimens, samples B and D; these latter porosities are very similar to the one of the material stored in pure water, sample A. The increase of porosity is a consequence of the sulfate attack and of the associate leaching process, this effect increases with the concentration of sodium sulfate of the solution. The measurements of mass density exhibit the same trend: the density is lower for samples C and D, which are affected by

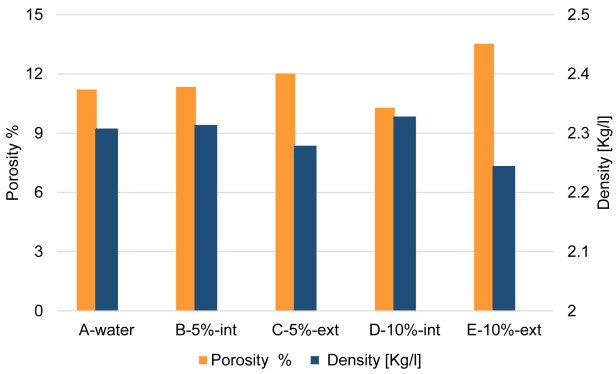

Figure 7: Porosity Incremental pore radius distribution and mass density (right axis) of mortar samples taken from concrete cylinders immersed in different solutions for 600 days

the sulfate attack.

Figure 8 compares the incremental pore distributions of samples D and E, taken from the internal and the external part of a concrete cylinder immersed in 10% sodium sulfate solution; the pore radius, expressed in μm is shown on the horizontal axis in a logarithmic scale, while the vertical axis report the incremental quantity of mercury infiltrated in the material at increasing pressure. The cumulative value for sample E is 36% higher than that of sample D, due to the increase of pores of small size, below 0.1 μm. From the incremental pore size distribution it can be seen that the majority of pores forming due to the sulfate attack have size between 0.01 and 0.1 μm.

5 Results on the overall specimens mechanical behavior

5.1 Mass uptake and expansion

As explained in Section 3, weight and expansion measurements were performed all along the three years of exposure of the specimens to the different solutions.

Figure 9 shows the mass variation in time for the specimens immersed in pure

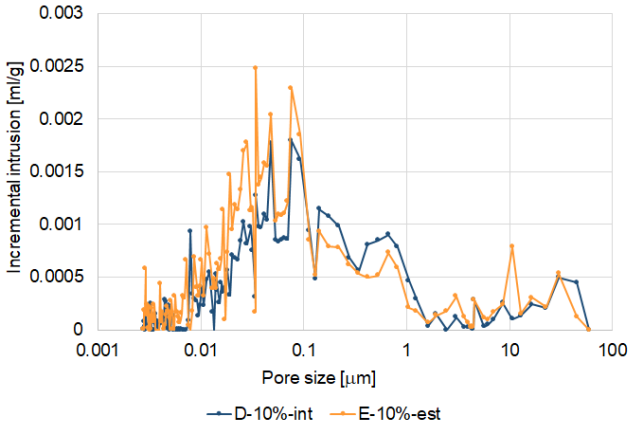

Figure 8: Incremental pore radius distribution in mortar samples taken from the internal and the external part of a concrete cylinder immersed in 10% sodium sulfate solution for 600 days

water and in sulfate solutions. Each curve represents the mean value of four cylinders, the bars represent the variance. In all cases a very similar constant value was reached after 3 months of immersion, denoting full saturation of the material.

The initial mean porosity of the concrete was computed as the ratio between the voids volume and the total volume of the cylinder. The voids volume was estimated by the volume that can be filled by water and computed from the difference between the mass of the fully saturated cylinder (after 3 months of immersion) and the mass of the same cylinder after drying for 6 months in a climatic chamber at $20°C$ and 50% relative humidity. The average value of porosity obtained was 0.18.

The displacement measurements of the distance between the studs in the longitudinal and radial directions allowed to characterize the time evolution of the specimens expansion which is due to both the water uptake and the chemical reactions.

Figures 10 and 11 show the time evolution of radial and longitudinal strains. Each curve represents the mean value of all the measurements for the 4 specimens stored in the same conditions (for each specimen, six measures in the

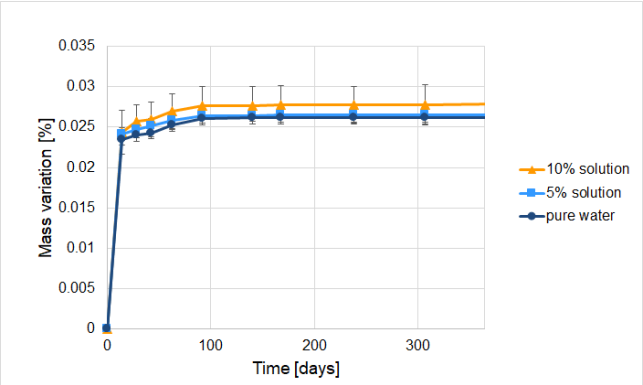

Figure 9: Mass variation of fully immersed cylinders: specimens in pure water, in 5% Na_2SO_4 solution and in 10% Na_2SO_4 solution

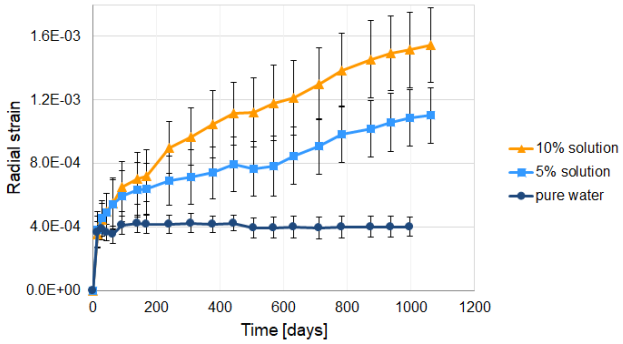

Figure 10: Radial strain of fully immersed cylinders: specimens in pure water, in 5% Na_2SO_4 solution and in 10% Na_2SO_4 solution

radial direction and four in the longitudinal direction for the first 500 days of test, a smaller number for the following part of the test).

The deformations of the specimens stored in water are due to the variation of the water content only and, hence, they stabilize when the specimens reach full saturation. The radial strain, Fig. 10, has a faster evolution than the longitudinal strain, Fig. 11, due to the geometry of the specimen. The samples stored in sulfate solutions with both concentrations exhibit a continuous growth of deformation in time due to the expansive chemical reactions occurring in the material. As confirmed by SEM observations presented in section 4.1, there is a delayed ettringite formation which causes swelling. The increase of deformation is higher in the radial direction because the ratio between the length of

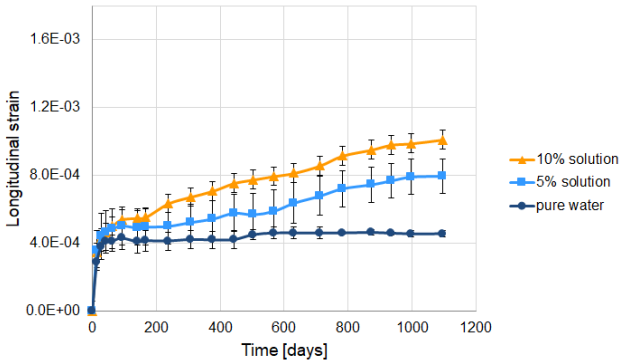

Figure 11: Longitudinal strain of fully immersed cylinders: specimens in pure water, in 5% Na_2SO_4 solution and in 10% Na_2SO_4 solution

the external layer where the reaction occurs and the total length is higher in that direction, as already observed in **?**. The variance of the radial strain is higher than the variance of longitudinal strain due to the different measurement procedure. In fact, while the probes of the mechanical comparator for longitudinal measures are inserted into the hole of the studs, the probes for the radial measures are just put in contact with the studs (see Figure 1).

The effect of the sulfate concentration of the solution is very clear: after three years of exposure in the 5% sodium sulfate solution the mean radial deformation is about 0.0011, while the specimens stored in the 10% solution have a mean radial deformation of about 0.0015. The same remark holds for the mean longitudinal deformation: 0.0008 for the specimens in the 5% solution and 0.0010 for those in the 10% solution.

The measured expansions are in the range of those reported in a paper just appeared **?** of an extensive experimental campaign on concrete prisms made with portland-limestone cements.

5.2 Compression tests on core samples

To characterize the possible mechanical degradation occurred after 3 years of exposure to sulfate solutions, some cores of 5 cm diameter were drilled from one cylinder stored in 10% sodium sulfate solution, one cylinder stored in 5%

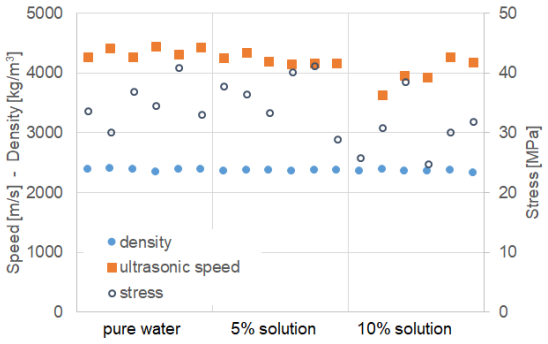

Figure 12: Ultrasonic speed (square symbols, left axis), density (round filled symbols, left axis) and compression strength (empty round symbols, right axis) after three years of immersion in pure water, 5% and 10% sodium sulfate solutions.

sodium sulfate solution and one cylinder stored in pure water for reference. For each cylinder, two cores were drilled very near to the lateral surface, where the penetration of sulfates is high, and one in the central part, where the effect of the SA is expected to be low. Two specimens, of length of 11 cm, were then obtained from each core.

Before performing the uniaxial compression tests on the specimens thus obtained, the material stiffness was indirectly measured by ultrasonic wave propagation tests. The measuring operation was performed in transparency using a transducer with frequency of 50 kHz, according to the standard UNI EN 12504-4:2001. Figure 12 shows the wave propagation velocity measured on the different specimens (square symbols, left axis). One can observe that the velocity is lower for the specimens coming from the cylinder stored in high concentration sodium solution. The wave propagation velocity depends on the density and on the stiffness of the material, to link the velocity decrease to the stiffness decrease and hence to the mechanical damage, one has to consider possible variations in mass density. The weight measurement showed that the density is uniform, see round filled symbols, left axis in Fig. 12.

Assuming a fixed value for the Poisson coefficient, the mean value of the dynamic elastic modulus is hence estimated through the following relation, La-

mond (2006)

$$E_d = V^2 \frac{[\rho(1+\nu)(1-2\nu)]}{(1-\nu)} \tag{1}$$

where: ρ = density of concrete; V = wave velocity; ν = Poisson's ratio; E_d = dynamic modulus of elasticity.

The relation between the static (E) and dynamic (E_d) elastic modulus of ordinary concrete can be obtained through the empirical correlation given by Lydon and Balendran (1986)

$$E = 0.83 E_d \tag{2}$$

The values thus obtained are shown in the histogram in Fig. 14. The dark blue bars represent the mean of the 6 specimens drilled from the same cylinder, while blue and light blue bars refer to the central (two specimens) and lateral (4 specimens) cores, respectively. For the concrete immersed in the 5% and 10% sulfate sodium solutions, one can observe a mean reduction of the Young modulus of 6.6% and 9.2%, respectively, with respect to that stored in water. For the specimens in 10% sulfate sodium solution, the damage is more pronounced in the cores near to the surface (ligth blue bars in Fig. 14) leading to a 21% stiffness reduction. Actually for cylinders immersed in the 10% sodium sulfate solution, macro-cracks in the circumferential direction formed, which were visible at the surface of the specimen before drilling the cores, see Figure 13. A similar pattern due to sulfate attack in concrete was also evidenced in **?**

The above ultrasonic measurements on cores confirm the findings of the porosimetry measurements and evidence that the penetration of sulfates leads to non-uniform strain in the cylindrical specimens with subsequent non-uniform degradation, as can be explained and predicted by reaction - diffusion models (see e.g. Tixier and Mobasher (2003), Cefis and Comi (2017)).

All specimens were then subject to uniaxial compression tests performed by an Instron testing machine with 100 kN servo-electric actuator. To measure the compression strength, half of the tests were performed by imposing a monotonously increasing displacement between the platens at rate of 3×10^{-6}

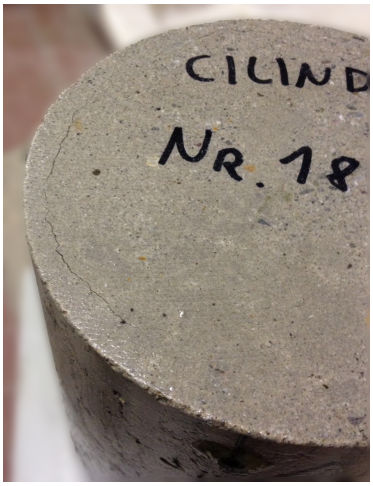

Figure 13: Circonferential crack on a specimen after two years of immersion in 10% Na_2SO_4 solution

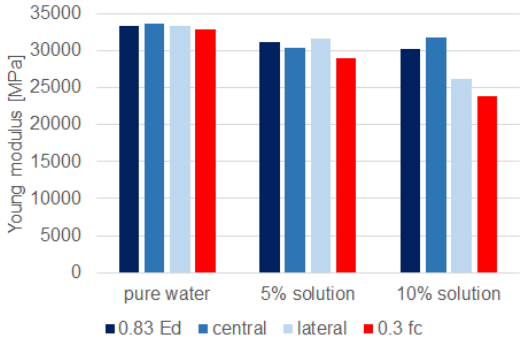

Figure 14: Modulus of elasticity after three years of immersion in pure water, 5% and 10% sodium sulfate solutions. Red bars correspond to the secant modulus E_s evaluated at $0.3f_c$ in compression tests on drilled cores, blue bars correspond to 0.83 of the dynamic modulus computed through ultrasonic tests (dark blue: mean values, blue: drilled cores from the central part of the specimens, light blue: drilled cores from the lateral part of the specimens).

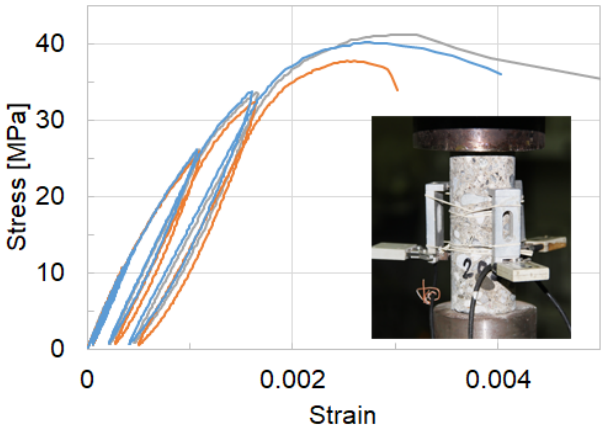

Figure 15: Stress vs strain response in compression tests on small cylinders drilled from the specimen after three years of immersion in 5% sodium sulfate solution; inset: experimental apparatus.

m/s and measuring the corresponding load by a load cell until rupture. To measure the Young modulus, the other tests were instrumented with three DD1 contact displacement transducers, of 50 mm measuring length, disposed at 120° on the lateral surface of the specimens (see inset in Fig. 15); some loading-unloading cycles were performed by imposing a non-monotonous displacement history, with linearly increasing and decreasing values, and a final linear growth until specimen failure. The compressive strength for all specimens is shown in Fig. 12 by empty circles, right axis. The values of strength obtained are 34.9 ± 3.7 MPa, 36.4 ± 4.6 MPa and 30.4 ± 4.9 for pure water, 5% and 10% sodium sulfate solutions, respectively. The cores extracted from the cylinder stored in the 10% solution thus showed a reduction of compression strength; however, one should observe that, due to the high heterogeneity of the cores, the dispersion of experimental strength is quite high. From the instrumented tests strain-stress curves can be obtained, as shown in Fig. 15. The Young modulus can then be estimated as the secant value corresponding to 0.3 of the material strength. The mean values thus obtained are reported in Fig. 14 (red bars). A reasonably good agreement is obtained with the ultrasonic measure and a significant decrease of the stiffness due to sulfate attack is confirmed.

6 Conclusions

This paper presents the results of laboratory tests lasted three years performed to investigate the degradation of a structural concrete exposed to external sulfate attack. Several different complementary chemo-physical and mechanical measurements have been conducted. The concrete was produced using a CEM II/A-LL, classified as sulfate resisting by several national codes; nevertheless, a significant effect of the sulfate attack was observed in specimens exposed to the solution with very high concentration, 10%, of sodium sulfate. After 400 days of immersion, the sulfates penetrated in the specimens through the porous microstructure and reacted with the aluminates of the cement paste, forming an expansive secondary phase, as evidenced by SEM-EDS and XRD analyses. The reaction also produced microcracks formation and a significant increase of the local porosity. Macroscopic measurements allowed to evidence the overall expansion of the specimens fully immersed in 5% and 10% sodium sulfate solutions all along the experimental campaign. After three years of immersion mechanical compression tests have been performed on cores drilled from the cylinders. A reduction of the Young modulus between 10% and 20% in the case of more aggressive solution was measured.

The present experimental observations show that the SA on concrete made by CEM II/A-LL produces a very significant expansion of the material, still evolving after three years. The comparison of mechanical properties of specimens stored in different solutions show that the degradation of compression strength and stiffness due to SA is quite limited, despite the high expansion registered. The stiffness degradation (in the range of 10% - 20%) obtained from both non-destructive ultrasonic measurements and by compression tests with unloading allows to identify the significant, but not critical, damage in the concrete specimen subject to SA. One should remark however that, since at this age the expansion is not yet stabilized, more severe damage could be observed at later ages; furthermore, at the structural level, the non-uniform expansion

may induce a change in the stress state that can cause further damage and macro-cracks formation.

Acknowledgements

The authors wish to thanks Prof. Maria Pia Riccardi for her help in realizing SEM-EDS observations and Marco Cucchi for compression tests.

Compliance with Ethical Standards

Conflict of Interest The authors declare that they have no conflict of interest.

References

Akpinar P, Casanova I (2010) A combined study of expansive and tensile strength evolution of mortars under sulfate attack: implications on durability assessment. Materiales de Costruccion 60-297:59–68

Alexander M, Bertron A, Editors NDB (2013) Performance of cement-based materials in aggressive aqueous environments. Springer

Bassuoni MT, Nehdi ML (2009) Durability of self-consolidating concrete to different exposure regimes of sodium sulfate attack. Mater Struct Constr 42(8):1039–1057

Boyd AJ, Mindess S (2004) The use of tension testing to investigate the effect of W/C ratio and cement type on the resistance of concrete to sulfate attack. Cem Concr Res 34(3):373–377

Brown P, Hooton R (2002) Ettringite and thaumasite formation in laboratory concretesprepared using sulfate-resisting cements. Cem Concr Compos pp 361–370

Cefis N, Comi C (2014) Damage modelling in concrete subject to sulfate attack. Fracture and Structural Integrity 29:222–229

Cefis N, Comi C (2017) Chemo-mechanical modelling of the external sulfate attack in concrete. Cement and Concrete Research 93:57–70

Chen J, Jiang M (2009) Long-term evolution of delayed ettringite and gypsum in portland cement mortars under sulfate erosion. Constr Build Mater 23:812–816

El-Hachem R, Rozière E, Grondin F, Loukili A (2012) Multi-criteria analysis of the mechanism of degradation of portland cement based mortars exposed to external sulphate attack. Cement and Concrete Research 42:1327–1335

EN197-1:2011 (2011) Cement - part 1: Composition, specifications and conformity criteria for common cements

Gong J, Cao J, Wang Y (2019) Effect of creep on the stress–strain relation of fly-ash slag concrete in marine environments. Structural Concrete pp 1–10

Haufe J, Vollpracht A (2019) Tensile strength of concrete exposed to sulfate attack. Cem Concr Res 116:81–88

Idiart A, Lopez C, Carol I (2011) Chemo-mechanical analysis of concrete cracking and degradation due to external sulfate attack: A meso-scale model. Cement and Concrete Research 33:411–423

Kakali G, Tsivilis S, Skaropoulou A, Sharp JH, Swamy RN (2003) Parameters affecting thaumasite formation in limestone cement mortar. Cem Concr Compos 25(8):977–981

Lamond J (2006) Significance of tests and properties of concrete and concrete-making materials. ASTM International 169

Loser R, Leemann A (2016) An accelerated sulfate resistance test for concrete. Mater Struct Constr 49(8):3445–3457

Lydon F, Balendran R (1986) Some observations on elastic properties of plain concrete. Cement and Concrete Research 16(3):314–324

Monteiro PJ, Kurtis KE (2003) Time to failure for concrete exposed to severe sulfate attack. Cement and Concrete Research 33(7):987 – 993

Naseer A, Jabbar A, Khan AN, Ali Q, Hussain Z, Mirza J (2008) Performance of pakistani volcanic ashes in mortars and concrete. Canadian Journal of Civil Engineering 35(12):1435–1445

Neville A (2004) The confused world of sulfate attack on concrete. Cement and Concrete Research 34:1275–1296

NPEN206-1:2007 (2007) Betão parte 1: Especificação, desempenho, produção e conformidade

Ouyang W, Chen J, Jiang M (2014) Evolution of surface hardness of concrete under sulfate attack. Construction and Building Materials 53:419–424

Park YS, Suh JK, Lee JH, Shing YS (1999) Strength deterioration of high strength concrete in sulfate environment. Cement and Concrete Research 29:1397–1402

Planel D, Sercombe J, Bescop PL, Adenot F, Torrenti J (2006) Long-term performance of cement paste during combined calcium leaching–sulfate attack: kinetics and size effect. Cement and Concrete Research 36(1):137–143

Rahman MM, Bassuoni MT (2014) Thaumasite sulfate attack on concrete: Mechanisms, influential factors and mitigation. Constr Build Mater 73:652–662

Ramezanianpour AM, Hooton RD (2013) Thaumasite sulfate attack in Portland and Portland-limestone cement mortars exposed to sulfate solution. Constr Build Mater 40:162–173, DOI 10.1016/j.conbuildmat.2012.09.104

Roziere E, Loukili A, Hachem RE, Grondin F (2009) Durability of concrete exposed to leaching and external sulphate attacks. Cement and Concrete Research 39:1188–1198

Santhanam M, Cohen M, Olek J (2003) Effects of gypsum formation on the performance of cement mortars during external sulphate attack. Cement and Concrete Research 33:325–332

Shamaa MA, Lavaud S, Divet L, Nahas G, Torrenti J (2015) Influence of relative humidity on delayed ettringite formation. Cement and Concrete Composites 58:14–22

Skalny J, Marchand J, Odler I (2002) Sulfate attack on concrete. Spon Press, London

Tixier R, Mobasher B (2003) Modeling of damage in cement-based materials subjected to external sulfate attack. J Mater Civ Eng 15:305–313

UNI9156:2015 (2015) Cementi resistenti ai solfati - classificazione e composizione

Yu C, Sun W, Scrivener K (2013) Mechanism of expansion of mortars immersed in sodium sulfate solutions. Cement and Concrete Research 43:105–111

List of Figures

List of Tables